

Alumina-Base Plasma-Sprayed Materials Part I: Phase Stability of Alumina and Alumina-Chromia

P. Chráska, J. Dubsky, K. Neufuss, and J. Písacka

Aluminum oxide is a relatively cheap, abundant material that is widely used for plasma-spray applications. This material, however, exists in many crystallographic modifications with different properties. In addition, most of these modifications are metastable and cannot be used in applications employed at elevated temperatures. Usually γ , δ , or other phases form after spraying, while α phase (corundum) is often the most desirable phase due to high corrosion resistance and hardness. This paper first reviews the method of α stabilization in the as-sprayed materials offered in literature. Then, as an example, it summarizes the results of an extensive study of chromia additions to alumina. Chromia was chosen because of its complete solid solubility in alumina and its crystal lattice type, which is similar to that of alumina. It was demonstrated that the addition of approximately 20 wt % chromia results in the formation of one solid solution of $(\text{Al-Cr})_2\text{O}_3$ in the α -modification.

Finally, this paper discusses the thermal stability of various alumina phases. Phase change routes of heating for different starting alumina modifications are discussed, and a case study of alumina-chromia is presented. Both types of as-sprayed structures, a mixture of α , δ , and γ phases, and 100% $(\text{Al-Cr})_2\text{O}_3$ were annealed up to 1300 °C and the phase composition checked. At lower temperatures and shorter holding times, the amount of α phase decreases while another metastable θ phase appears, and the fraction of $\gamma + \delta$, if present, increases. At temperature above 1100 °C, the amount of α phase increases again.

Keywords alumina, oxide ceramics, phase composition, temperature stability

1. Introduction

Aluminum oxide was one of the first materials used for plasma spraying (PS). However, as requirements for coating properties increased, alumina often was not able to satisfy them, especially for applications at elevated temperatures. Therefore, attention shifted to zirconia, where stabilized forms were developed (partially-stabilized zirconia [PSZ], fully-stabilized zirconia [FSZ]) (Ref 1, 2), and to other materials. The insufficiency of alumina deposits in most cases is caused by alumina polymorphism, which causes its instability. Aluminum oxide is a complex material even in the massive, bulk form and exhibits various phases such as the hard, stable trigonal α (corundum). This phase is often accompanied by hexagonal β ($\text{Me}_x\text{O} \cdot \gamma\text{Al}_2\text{O}_3$, where Me: Ca, Ba, Sr, K, Li, etc. and mainly Na) as an aluminate, a defective spinel cubic $\gamma\text{Al}_2\text{O}_3$, a deformed tetragonal spinel $\delta\text{Al}_2\text{O}_3$, a high temperature hexagonal phase $\epsilon\text{Al}_2\text{O}_3$, a monoclinic $\theta\text{Al}_2\text{O}_3$ where Al^{3+} forms octahedric chains in a cubic oxygen sublattice, and some other phases occurring rarely (ν , ι , χ , κ ...). Reference 3 provides a full description.

The situation can be even more complex after PS. The microstructure of sprayed alumina consists of a series of overlapping lamellae produced by the splat cooling of impinging droplets. Due to generally very rapid but sometimes different quenching

and solidification rates of various parts of PS deposits, different phases can be found. Depending on the feedstock powders, geometrical set up of PS, and cooling rates of deposits (often related to their thickness), some coatings exhibit a thin amorphous layer next to the substrate, followed by various crystalline layers, which often reveal nonequilibrium (and even nonstoichiometric) phases (Ref 4, 5).

The crystallographic phase composition of PS alumina is strongly related to the cooling rate. In 1957, Ault (Ref 6) showed that γ phase formed in deposits, regardless of the α -modification of the starting powder. Generally, the higher the cooling rate, the more the γ phase (Ref 4, 5, etc.). Conversely, free flight particles caught in water are cooled significantly more slowly than those on a cold substrate ($10^4 \text{ K} \cdot \text{s}^{-1}$ compared to $10^6 \text{ K} \cdot \text{s}^{-1}$ on average). The time available for the transformation is longer, and the δ phase is formed predominantly (Ref 7). Smaller particles (droplets) also contain γ phase in addition to the δ phase, and larger droplets have exhibited $\alpha\text{Al}_2\text{O}_3$. Both phases (γ , δ) are metastable and their changes to stable α , usually the most desirable in deposits due to its high corrosion and erosion resistances, and hardness, are accompanied by a significant volume change ($\gamma \rightarrow \alpha$ volume change is $\approx 15\%$) which results in microcrack formation and attendant problems.

Although the phase transformations in alumina-base ceramics were described in several papers, most dealt with bulk materials. Additional heat treatment processes for the production of a desirable phase are often costly and usually lead to deterioration of other properties. All producers try to avoid them and to find other methods for transformation temperature control. One method is an induced heterogeneous nucleation by foreign nuclei— $\alpha\text{Al}_2\text{O}_3$ (Ref 8, 9, 10), $\gamma\text{Al}_2\text{O}_3$ (Ref 10), or $\alpha\text{Fe}_2\text{O}_3$ (Ref 9, 11, 12). Tushida et al. (Ref 12) described a binary system where

P. Chráska, J. Dubsky, K. Neufuss, and J. Písacka, Institute of Plasma Physics, Academy of Sciences, Prague 8, Czech Republic.

low melting point V_2O_5 added to Al_2O_3 markedly lowered the interfacial energy by formation of $AlVO_4$ phase and enhanced element redistribution.

The transformation temperature can also be modified by cations of some metals. For example, Bye and Sympkin (Ref 11) studied the effect of chromium and iron on the formation of α and γAl_2O_3 . Addition of less than 4 wt% Cr_2O_3 to aluminum oxide results in the formation of θAl_2O_3 , with no influence on further transformation to the α phase. Bonder et al. (Ref 13) found that chromium lowered the crystallization temperature for γAl_2O_3 and increased the $\gamma \rightarrow \alpha$ transformation temperature significantly more than iron addition.

The previous examples illustrate the importance of investigating the phase stability and phase changes or methods of phase stabilization during the plasma spraying of alumina-base ceramics.

2. Stabilization of Alpha Alumina in As-Sprayed Materials

2.1 Previous Results

McPherson, who pioneered studies on stabilization of alumina (Ref 14, 15), showed that when α particles are only partially melted, their unmelted cores can act as nuclei for α formation and, consequently, the volume of the α phase after plasma spraying can be substantially increased (Ref 14). Two other methods of increasing the α phase content after PS discussed by McPherson are preheating of the substrate to a temperature above 900 °C or an additional heat treatment of deposits at 1100 °C. Both methods, however, lead to deterioration of the substrate properties. McPherson, using results of the precise structural studies (Ref 16, 17, 18) and on the basis of experimental work on Al_2O_3 with 24 wt% Cr_2O_3 (Ref 15), concluded that in the dominantly formed θ phase (with only traces of δ and α phases), ions of Al^{3+} are equally distributed in the tetrahedral and octahedral positions of a rotated close packed cubic lattice of the oxygen anions. Cations of Cr^{6+} in θAl_2O_3 occupy only octahedral positions due to high octahedral stabilization energy. The location of Al^{3+} cations in the lattices of γAl_2O_3 and δAl_2O_3 , predominantly in the octahedral sites in the cubic close packed lattice of oxygen anions in the spinel, corresponds to distribution of aluminum ions in the melt (Ref 19). There is little time available for cation redistribution and γ phase forms because this phase has a lower nucleation energy than the αAl_2O_3 due to a lower energy of the solid-liquid interface (Ref 20). This is true for temperatures up to approximately 1700 °C; at higher temperatures the α phase nucleates easily. Reference 21 reports a similar critical temperature.

Meyer (Ref 22) reports that 5% of Cr_2O_3 in Al_2O_3 forms a solid solution and appears either green in the γ -modification or red in the α phase. Preheating of the substrate to 1000 °C results in poor deposit properties, and Meyer suggests cooling the coatings below that temperature. Barry et al. (Ref 23) prepared a mixture of $Al_2O_3 + Cr_2O_3$, using the plasma technique, from a mixture of CrO_2Cl_2 and $AlCl_3$. The resulting powder consisted of δ and θ modifications. The maximum solubility limit of Cr_2O_3 according to Barry et al. (Ref 23) was 5 to 6 wt% in the solid solution, with excess chromium oxide in the form of hex-

agonal plates. McPherson (Ref 15) observed the solubility limit of Cr_2O_3 in the θAl_2O_3 as 18 wt%. Significant changes of αAl_2O_3 lattice parameters with the Cr_2O_3 content were observed by Davies et al. with maximum at 7 wt% (Ref 24). The mutual solubility of both oxides in the equilibrium is generally very good with the exception of a miscibility gap below 950 °C. However, the nonequilibrium conditions of the plasma-spray process result in several other peculiarities: solubility of TiO_2 or Y_2O_3 in Al_2O_3 and precipitation at an additional heat treatment (Ref 25), volatilization of Cr_2O_3 during the spraying, formation of α solid solution for 50 wt% Cr_2O_3 , or the existence of an amorphous phase in Al_2O_3 with 34 to 64 wt% ZrO_2 in the Al_2O_3 system (Ref 26).

2.2 Stabilization of Alpha Alumina by Chromia

2.2.1 Experimental

Chromia (Cr_2O_3) was selected as an addition to alumina because it exhibits complete solid solubility and has a crystal lattice type that is similar to Al_2O_3 . All deposits (coatings and free-standing parts) were made using the water-stabilized plasma torch WSP PAL 160 (Institute of Plasma Physics, Prague). Details of the experimental techniques are given elsewhere (Ref 27) with a description of the feedstock powder preparation (Table 1). All feedstock powders, free-flight particles (caught in water after PS), and deposits were compared on the basis of structure, phase composition, and chemical homogeneity (Ref 28).

2.2.2 Results and Discussion

Tables 1 and 2 summarize the main data on the feedstocks and the as-sprayed deposits. Figure 1 shows the x-ray diffraction

Table 1 Feedstock powders

Sample code	Cr_2O_3 , wt %	Phases present	Particle size, μm
AB5	0.0	αAl_2O_3	63 to 90
AC0	1.4	αAl_2O_3	63 to 90
A1C	9.1	γAl_2O_3 , Cr_2O_3	63 to 100
A2C	19.1	γAl_2O_3 , θAl_2O_3 , Cr_2O_3	36 to 90
A3C	26.8	αAl_2O_3 , Cr_2O_3	40 to 120
A5C	37.1	γAl_2O_3	63 to 100

Table 2 Phase composition and thickness of the as-sprayed samples

Sample code	Thickness, μm	α phase wt %	Other phases
AB5	610	8.1	γAl_2O_3 , δAl_2O_3
AC0	520	6.4	γAl_2O_3 , δAl_2O_3
A1C	150	67.1	γAl_2O_3 , δAl_2O_3 , traces Cr_2O_3
A2C	150	100	...
A3C	60	100	...
A5C	30	100	...

(XRD) patterns of the as-sprayed deposits. From these results, it is evident that chromia aids in the formation of the α form of alumina at the expense of γ and δ phases in feedstock. Secondly, it is apparent that the dwell time above the melting temperature of both oxides during spraying is sufficiently long for the mutual dissolution of both components and the formation of $(Al-Cr)_2O_3$ solid solution, even for the highest chromia concentration. This was also shown by the linear plot of measured interplanar spacings of $(113)_\alpha$ with respect to chromia content, corresponding to Vegard's law (Ref 28). No traces of metallic chromium were found in deposits by chemical microanalysis, and no chromia

was indicated by XRD. These results are contrary to solid solubility limits (5 to 6 wt% [Ref 23] and 18 wt% [Ref 15]) and to the findings of Costa et al. (Ref 29) that showed metallic chromia in deposits. However, minute amounts of γ phase in some samples cannot be entirely excluded where their presence is masked because the intensities and deformations of $(202)_\alpha$ and $(124)_\alpha$ lines coincide with the $(400)_\gamma$ and $(440)_\gamma$ lines. It can be concluded that the shift of α lines and the non-existence of distinct chromia and metallic chromia phases support a process where aluminum is substituted in the lattice by chromium cations (Ref 30).

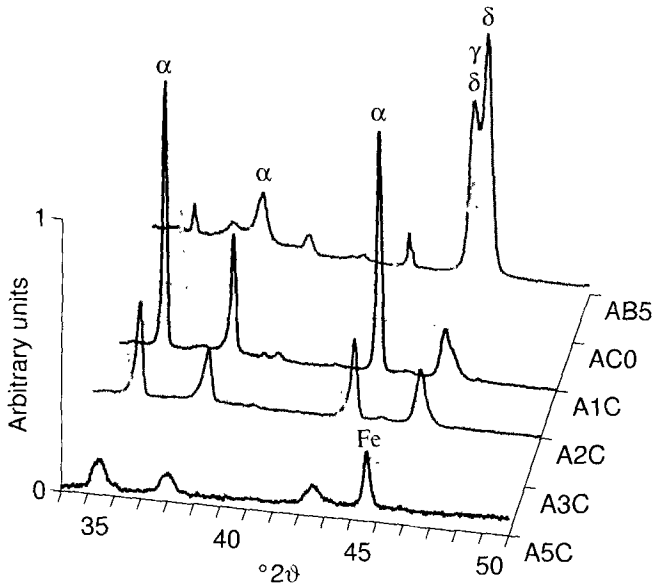


Fig. 1 XRD patterns of the as-sprayed samples (CuK α)

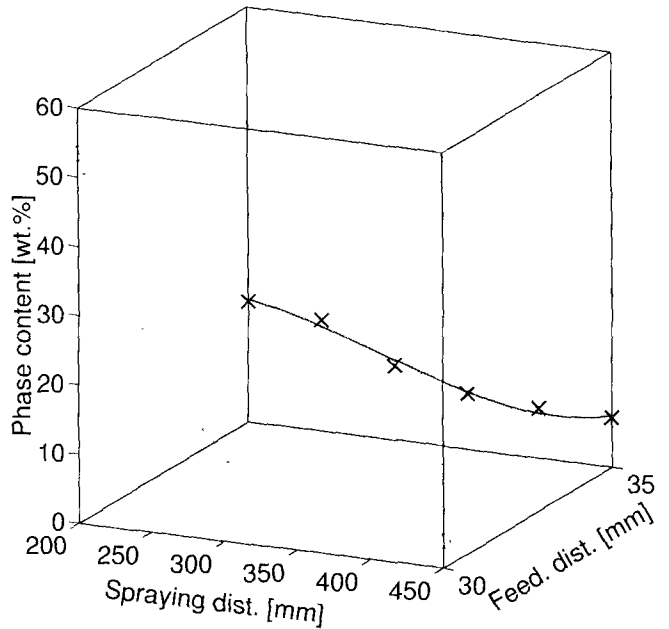


Fig. 2 Dependency of α phase content on spraying parameters for pure alumina

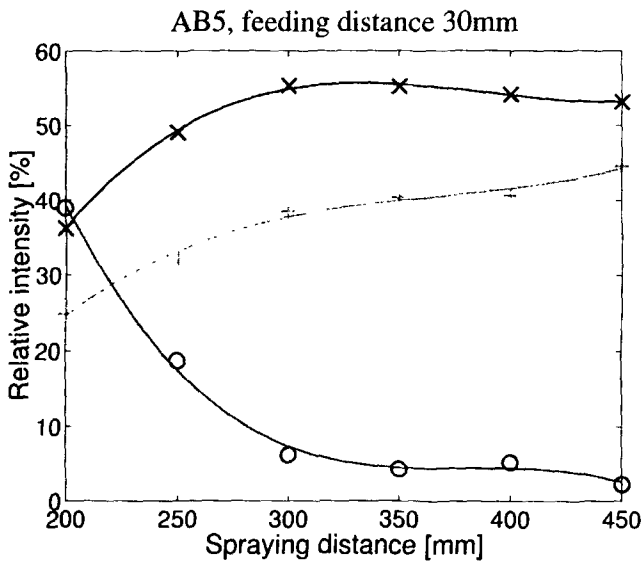


Fig. 3 Dependency of XRD relative intensities on spraying distance for pure alumina AB5. \circ = $(113)_\alpha$, $+$ = coinciding $(400)_\gamma$ and $(400)_\delta$, \times = $(0012)_\delta$

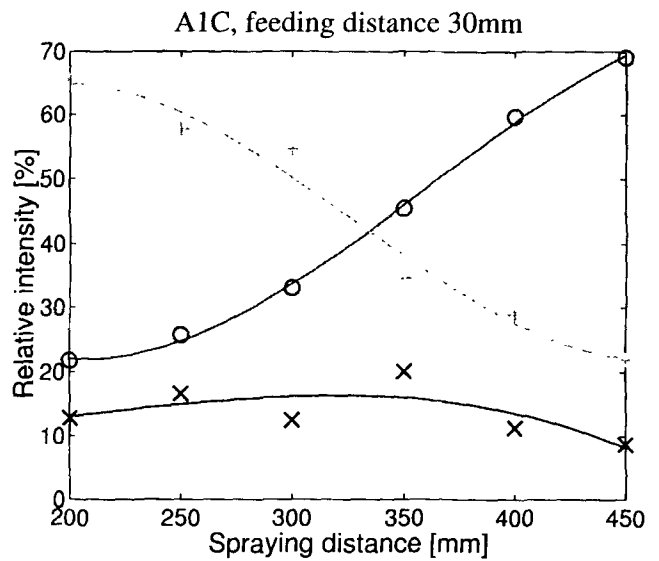


Fig. 4 Dependency of XRD relative intensities on spraying distance for alumina-chromia A1C. \circ = $(113)_\alpha$, $+$ = coinciding $(400)_\gamma$ and $(400)_\delta$, \times = $(0012)_\delta$

2.3 Effect of PS Parameters on Formation of Alpha Phase

This section indicates that the amount of α corundum in as-sprayed materials can be controlled by methods other than solely changing the chemical composition. However, it is necessary to consider that while “chemical stabilization” is independent of the PS system, control through changes of the spraying parameters and PS set up cannot be generalized as such but is specific to a certain spraying system. The results presented here were obtained for spraying with WSP PAL 160 where, besides choosing the spraying distance (SD) (also referred to as the

stand-off distance), the position of the powder injector can be easily changed (i.e., the feeding distance [FD]).

McPherson examined the effect of parameters on the phase composition of alumina (Ref 31). More recently, the dependency of B-Y₂O₃ formation on the torch-substrate distance (Ref 32) was demonstrated.

Details of the experimental work and discussion of results are given elsewhere (Ref 33, 34). Figures 2 and 3 indicate that for SD up to approximately SD = 300 mm with FD = 30 mm, alumina particles are probably only partially melted and then act as nuclei for α formation in the deposits. Later they are fully melted and, therefore, predominantly $\gamma + \delta$ phases are formed in

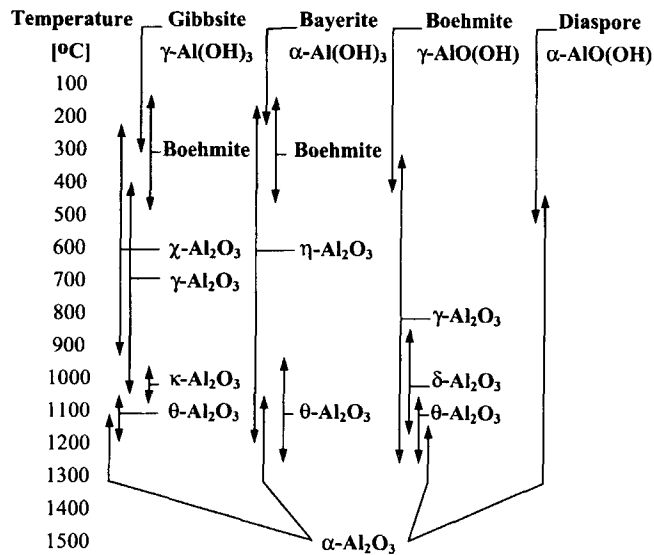


Fig. 5 Aluminum hydroxides decompositions. (Lines with arrows indicate the corresponding temperature ranges)

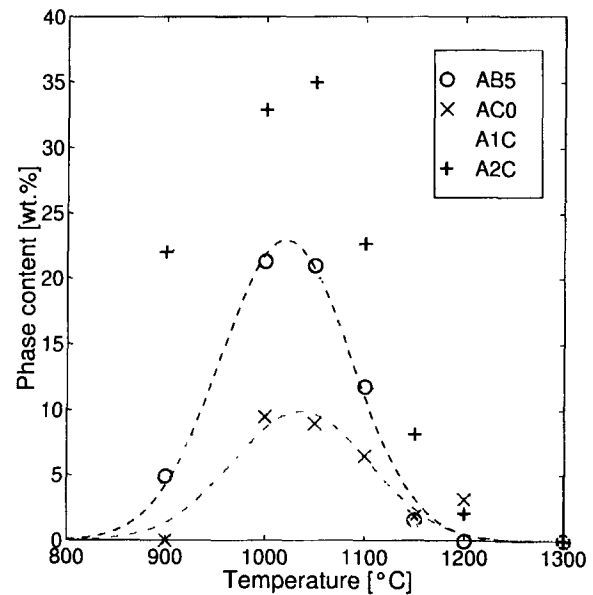


Fig. 6 Content of metastable θ phase in dependency on the annealing temperature for the longest holding time

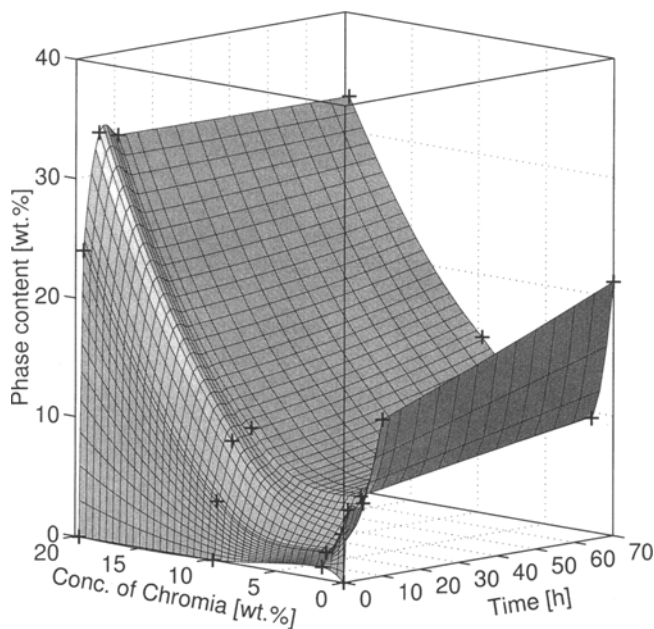


Fig. 7 Dependency of θ phase content on chromia composition and time for 1000 °C

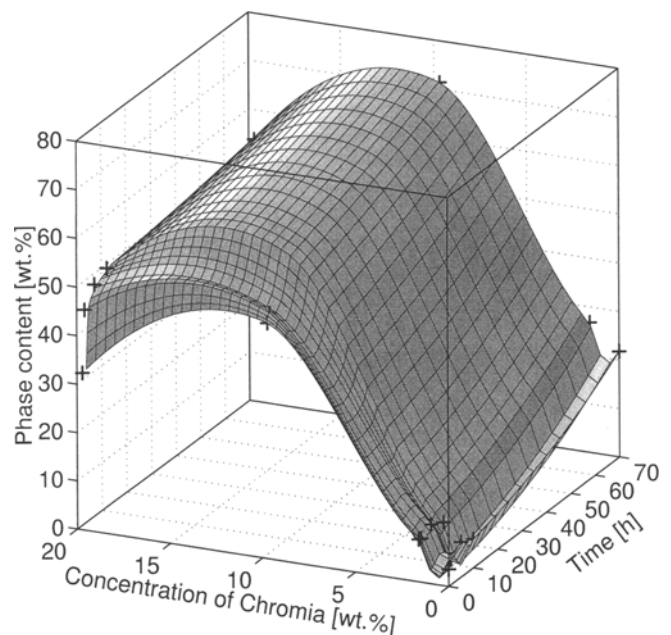


Fig. 8 Kinetics diagram of α phase content for 1000 °C

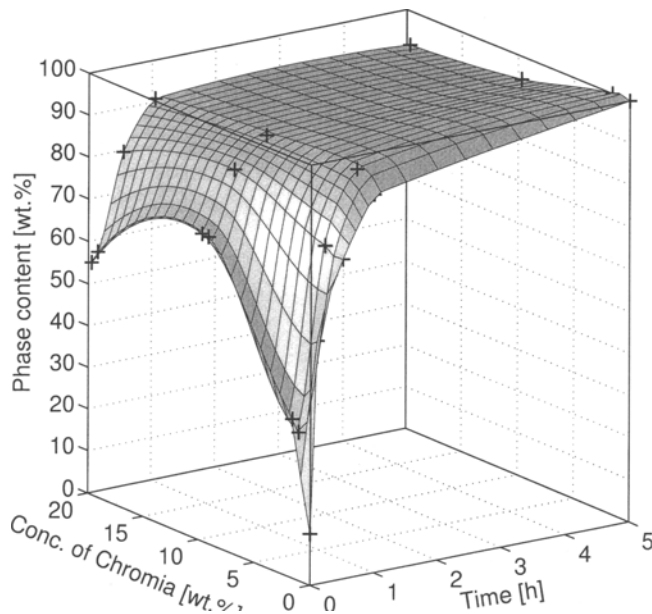


Fig. 9 Kinetics diagram of α phase content for 1200 °C

Feedstock powder	$\alpha - \text{Al}_2\text{O}_3$	
Coating	$\gamma + \delta$	(α)
Annealing	γ δ	(α)
< 900 °C	δ	(α)
900 °C	θ	(α)
1 000 °C	$\alpha - \text{Al}_2\text{O}_3$	(α)

Fig. 10 Transformation sequence for the as-sprayed alumina on annealing

deposits. A small amount of chromia allows the amount of α phase to steadily grow with SD (Fig. 4). There is sufficient time for enhanced mixing of chromia with alumina, which results in α stabilization.

3. Thermal Stability of Alumina-Base Materials

3.1 Decomposition of Aluminum Hydroxides on Annealing

A general chart on the decomposition of aluminum hydroxides (Fig 5) illustrates the complicated nature of alumina phase

transitions. For instance, on annealing Gibbsite, five transition metastable phases are formed prior to $\alpha\text{Al}_2\text{O}_3$. Also, the temperature ranges of various phases (as indicated by solid lines with arrows) can overlap depending on parameters such as heating or cooling rates, particle size, etc.

3.2 Annealing of Alumina-Base Deposits

3.2.1 Experimental

The same samples (Table 1) and techniques described in section 2.2 were used for thermal stability studies. The annealing was performed in evacuated quartz capsules at 900 to 1300 °C with holding times from 5 to 150 h to reach a near-equilibrium state of the structure. References 27, 28, and 30 provide further details.

3.2.2 Results and Discussion

In addition to α , γ , and δ phases present in the as-sprayed samples, another metastable phase, θ , forms on annealing. Figure 6 shows the dependence of θ content on annealing temperatures for the longest holding times. An example of the kinetics, that is, the time dependency of the θ phase content for 1000 °C, is given in a three-dimensional diagram (Fig. 7). Chromia concentration influences the α phase content after annealing. Data from the quantitative analysis were used for construction of three-dimensional kinetics diagrams (Fig. 8, 9). It was found that around 900 °C, the as-sprayed mixture of α , γ , and δ (if present) decomposes and θ is formed, which in turn transforms to α . However, the amount of α does not reach the same value as in the as-sprayed state for annealing temperatures below 1300 °C and 5 h holding times. For annealings from this temperature and above, all phases present in deposits transform to the α phase, and no traces of other phases were detected (Ref 30, 35). However, under certain conditions, the as-sprayed $\alpha(\text{Al,Cr})_2\text{O}_3$ could decompose into two phases (a stable and an unstable phase, denoted α and α'). Similarly, two different $\theta + \theta'$ and $\delta + \delta'$ phases can evolve. Figure 10 summarizes the transformation sequence for the as-sprayed pure alumina, and Fig. 11 summarizes the sequence for the as-sprayed alumina-chromia.

Several authors (Ref 14, 36) have suggested that aluminum ions in θ phase are located equally at tetrahedral and octahedral positions of the oxygen lattice, and that chromium ions are located only in the octahedral positions. At the equilibrium $\alpha\text{Al}_2\text{O}_3$, aluminum ions are at the octahedral positions of a hexagonal close packed lattice (Ref 37). The results suggest that aluminum and chromium ions cannot always occupy the equilibrium positions, and the phases formed are, therefore, not fully stable. Necessary redistribution can materialize only when the mobility of both ions is increased by annealing. These processes can be partially affected by the slightly nonhomogeneous distribution of chromium in $(\text{Al-Cr})_2\text{O}_3$ (Ref 28) and by the preferred orientation of the columnar crystals in splats.

4. Conclusions

- Crystallographic phase composition of PS alumina is related to the cooling rate of the deposit. After spraying of

Feedstock powder $\text{Al}_2\text{O}_3 + \text{Cr}_2\text{O}_3$ -

Coating

$\alpha + \delta + \gamma$

Annealing

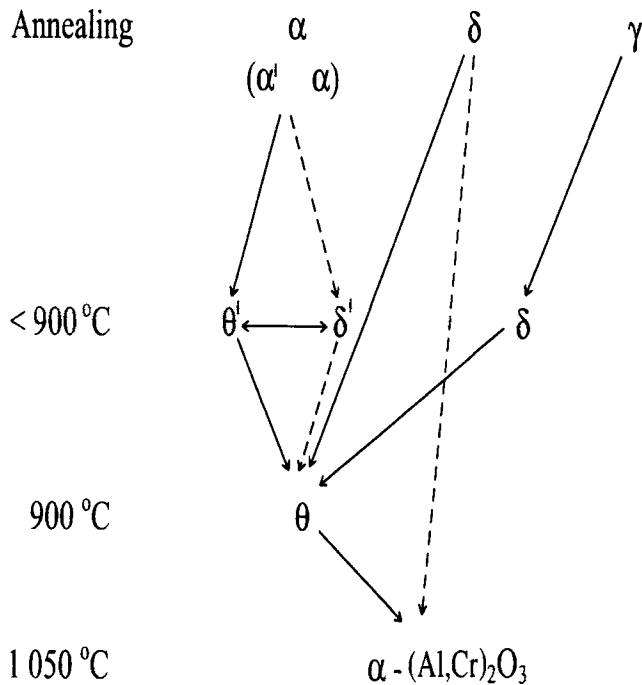


Fig. 11 Transformation sequence for the as-sprayed alumina-chromia on annealing. α , γ , δ , θ are stable phases $(\text{Al,Cr})_2\text{O}_3$ type and α' , δ' , θ' are unstable phases $(\text{Al,Cr})_2\text{O}_3$ type

alumina, γ or δ phases usually form. The α phase is the most desirable.

- Additional heat treatment of PS alumina deposits is not a solution for production of the desirable α phase, mainly due to the appearance of several transition phases during this process.
- It was demonstrated that the addition of 20 wt% Cr_2O_3 results in formation of one solid solution after PS, $(\text{Al-Cr})_2\text{O}_3$, which is in the α modification.

Acknowledgments

This work was partially supported by the grants GACR 106/93/0638 and GACR 202/95/0216.

References

1. R.C. Garvie, R.H. Hannink, and R.T. Pascoe, Ceramic Steel?, *Nature*, Vol 258, 1975, p 703-704
2. J.R. Brandon and R. Taylor, Thermal Properties of Ceria and Ytria Partially Stabilized Zirconia Thermal Barrier Coatings, *Surf. Coat. Technol.*, Vol 39, 40, 1989, p 143-151
3. Powder Diffraction File, Alphabetical index, JCPDS, International Centre for Diffraction Data, PA, USA, 1986
4. P. Chráska, J. Dubsky, B. Kolman, J. Ilavsky, and J. Forman, Study of Phase Changes in Plasma Sprayed Deposits, *J. Therm. Spray Technol.*, Vol 1 (No. 4), 1992, p 301-306
5. C.X. Ding, R.A. Zatorski, and H. Herman, Oxide Powders for Plasma Spraying—The Relationship between Powder Characteristic and Coating Properties, *Thin Solid Films*, Vol 118, 1984, p 467-475
6. N.N. Ault, Characteristics of Refractory Oxide Coatings Produced by Flame-Spraying, *J. Am. Ceram. Soc.*, Vol 40 (No. 3), 1957, p 69-74
7. J. Dubsky, B. Kolman, and P. Chráska, The Influence of Cooling Rate on Phase Transformations in Al_2O_3 , *Proc. of 7th Metallographic Symposium*, Part 1, J. Šujan, Ed., CSVTS Košice, Vysoké Tatry, Czechoslovakia, 1989, p 168-171
8. M. Kumagai and G.L. Messing, Enhanced Densification of Boehmite Sol-Gels by α -Alumina Seeding, *J. Am. Ceram. Soc.*, Vol 67, 1984, C230-231
9. Y. Suwa, R. Roy, and S. Komarneni, Lowering Crystallization Temperatures by Seeding in Structurally Diphasic Al_2O_3 -MgO Xerogels, *J. Am. Ceram. Soc.*, Vol 68, 1985, C238
10. G.L. Messing, M. Kumagai, R.A. Shellman, and J.L. McArdle, Seeded Transformation for Microstructural Control in Ceramics, *The Science of Ceramic Chemical Processing*, L.L. Hench and D.R. Ulrich, Ed., Wiley, 1986, p 259-271
11. G.C. Bye and G.T. Sympkin, Influence of Cr and Fe on the Formation of α - Al_2O_3 from γ - Al_2O_3 , *J. Am. Ceram. Soc.*, Vol 57, 1974, p 367-371
12. T. Tushida, R. Furuichi, T. Ishii, and K. Itoh, The Effect of Cr^{3+} and Fe^{3+} Ion on the Transformation of Different Aluminum Hydroxides to α - Al_2O_3 , *Thermochim. Acta*, Vol 64, 1983, p 337-353
13. I.A. Bonder, V.B. Glushkova, and P.A. Ceitlin, Study of Phase Changes in Al_2O_3 , *Neorg. Mater.*, Vol 7, 1971, p 1367-1371
14. R. McPherson, On the Formation of Thermally Sprayed Alumina Coatings, *J. Mater. Sci.*, Vol 15, 1980, p 3141-3149
15. R. McPherson, The Structure of Al_2O_3 - Cr_2O_3 Powders Condensed from a Plasma, *J. Mater. Sci.*, Vol 8, 1973, p 859-862
16. B.C. Lippens and J.H. DeBoer, Study of Phase Transformations During Calcination of Aluminum Hydroxides by Selected Area Electron Diffraction, *Acta Crystallogr.*, Vol 17, 1964, p 1312
17. G. Ervin, Structural Interpretation of the Diaspore-Corundum and Boehmite- γ - Al_2O_3 , *Acta Crystallogr.*, Vol 5, 1952, p 103-108
18. A.M. Lejus, Metastable Phases Formation in Aluminum Hydroxides, *Rev. Int. Hautes. Temp. Refract.*, Vol 1, 1964, p 53-59
19. A. Nukui, H. Tagai, H. Morikawa, and S.I. Iwai, Structural Conformation and Solidification of Molten Alumina, *J. Am. Ceram. Soc.*, Vol 59, 1976, p 534
20. R. McPherson, Formation of Metastable Phases in Flame- and Plasma-Prepared Alumina, *J. Mater. Sci.*, Vol 8, 1973, p 851-858
21. F.B. Vurzel, V.A. Khmel'nik, V.F. Nazarov, and G.V. Kosoruchkin, Production of Thermally Deposited Aluminas, *Phys. Chem. Mater. Treat.*, (Russia), Vol 3, 1988, p 86-91
22. H. Meyer, On the Application of Chromium Oxide-Containing Alumina to Flame Spraying, *Ber. Deutsche Keramik. Ges.*, Vol 40, 1963, p 385
23. T.I. Barry, R.K. Bayliss, and L.A. Lay, Mixed Oxides Prepared with an Induction Plasma Torch, Part I Chromia/Alumina, *J. Mater. Sci.*, Vol 3, 1968, p 229-238
24. T.J. Davies, H.G. Emblem, C.S. Nwobodo, A.A. Ogwn, and V. Tszatzalou, Preparation and Properties of Some Alumina-Chrome Refractories, *J. Mater. Sci.*, Vol 26, 1991, p 1061
25. S. Safai and H. Herman, Plasma-Sprayed Materials, *Treat. Mater. Sci. Tech.*, Vol 20, 1981, p 183-214
26. A. Krauth and H. Meyer, Modifications Produced by Chilling and Their Crystal Growth in the System Containing Zirconium Dioxide, *Ber. Deutsche Keramik. Ges.*, Vol 42, 1965, p 61-72
27. J. Dubsky, V. Brozek, B. Kolman, and P. Chráska, Stabilization of α - Al_2O_3 by Chromia, Ceramics Adding the Value, *Proc. of the Inter. Ceram. Conf. AUSTCERAM 92*, Vol 2, M.J. Bannister, Ed., CSIRO, Australia, 1992, p 793-797

28. J. Dubsky, B. Kolman, V. Brozek, and P. Chráska, The Chemical Inhomogeneity of $\text{Al}_2\text{O}_3\text{-Cr}_2\text{O}_3$ Powders for Plasma Spraying, *Proc. of 16th Symposium on Plasma Physics and Technology*, Czech Technical University, Prague, Czechoslovakia, 1993, p 267-273
29. V. Costa, C. Pacheco de Silva, T. Puig, and A.M. Dias, Influence of H.I.P. and Laser Treatments on Ceramic Plasma Sprayed Coatings, *Proc. 2nd Plasma-Technik-Symposium*, Vol 1, Luzern, Switzerland, 1991, p 363-372
30. J. Dubsky, B. Kolman, and P. Chráska, Stability of Alpha Phase in Alumina-Chromia Plasma Sprayed Deposits After Annealing, *1994 Thermal Spray Industrial Applications*, C.C. Berndt and S. Sampath, Ed., ASM International, 1994, p 779-782
31. R. McPherson, Formation of Metastable Monoclinic Rare Earth Sesquioxides from the Melt, *J. Mater. Sci.*, Vol 18 (No. 5), 1983, p 1341-1345
32. V. Gourlaouen, G. Schnedecker, A. Grimaud, P. Fauchais, A.M. Lejus, and R. Collengues, Metastable Phase in Yttrium Oxide Plasma Spray Deposits and Their Effect on Coating Properties, *1994 Thermal Spray Industrial Applications*, C.C. Berndt and S. Sampath, Ed., ASM International, 1994, p 615-619
33. J. Ilavsky, K. Neufuss, and P. Chráska, Influence of Spraying Parameters on Properties of Al_2O_3 Deposits, *Proc. of 5th Conference on Aluminum Oxide*, Prague Institute of Chemical Technology, Prague, Czech Republic, 1990, p 65-70
34. J. Dubsky, B. Kolman, and P. Chráska, Effect of Spraying Parameters on Phase Composition of Deposits Prepared by the WSP Process, *1995 Advances in Thermal Spray Science & Technology*, C.C. Berndt and S. Sampath, Ed., ASM International, 1995, p 421-424
35. J. Dubsky, B. Kolman, and J. Forman, High-Temperature Stability of Plasma Sprayed Al_2O_3 Coatings, *Proc. of 1st Czech National Thermal Conference*, J. Musil, J. Kubíček, and S. Korcák, Ed., Technical University Brno, Czech Republic, 1994, p 150-153
36. W.D. Kingery, *Introduction to Ceramics*, J. Wiley, 1960, p 566
37. S.J. Geller, Crystal Structure of $\beta\text{-Ga}_2\text{O}_3$, *J. Chem. Phys.*, Vol 33, 1960, p 676-681